$\Lambda_c(2910)$ and $\Lambda_c(2940)$ as conventional baryons dressed with the D^*N channel

Zi-Le Zhang [1,2] Zhan-Wei Liu [1,2,3,*] Si-Qiang Luo, [1,2,3,†] Fu-Lai Wang, [1,2,3,‡]
Bo Wang [4,5,6,§] and Hao Xu [7,8,‖]

[1]*School of Physical Science and Technology, Lanzhou University, Lanzhou 730000, China*
[2]*Research Center for Hadron and CSR Physics, Lanzhou University and Institute of Modern Physics of CAS, Lanzhou 730000, China*
[3]*Lanzhou Center for Theoretical Physics, Key Laboratory of Theoretical Physics of Gansu Province, and Frontiers Science Center for Rare Isotopes, Lanzhou University, Lanzhou 730000, China*
[4]*School of Physical Science and Technology, Hebei University, Baoding 071002, China*
[5]*Key Laboratory of High-precision Computation and Application of Quantum Field Theory of Hebei Province, Baoding 071002, China*
[6]*Research Center for Computational Physics of Hebei Province, Baoding, 071002, China*
[7]*Institute of Theoretical Physics, College of Physics and Electronic Engineering, Northwest Normal University, Lanzhou 730070, China*
[8]*Lanzhou Center for Theoretical Physics, Lanzhou University, Lanzhou 730000, China*

In this work, we treat $\Lambda_c(2910)^+$ and $\Lambda_c(2940)^+$ as the conventional udc cores dressed with the D^*N channel. We provide a possible interpretation to both $\Lambda_c(2910)^+$ and $\Lambda_c(2940)^+$ within the same framework. In the study, we consider not only the effects between the conventional triquark core and the D^*N channel but also the D^*N-D^*N interactions. The mass of the Λ_c state with $J^P = 1/2^-$ is larger than that with $J^P = 3/2^-$ in this unquenched picture, which is very different from the prediction of the conventional quenched quark model. Based on the mass spectrum, the spin parity of $\Lambda_c(2940)^+$ is more likely to be $1/2^-$, while $\Lambda_c(2910)^+$ prefers $3/2^-$. We look forward to the future experiments that can test our results with more precise experimental data.

I. INTRODUCTION

Until now, a growing number of charmed baryons have been reported with the accumulation of experimental data [1]. Many of them can properly fit into the conventional charmed baryon spectrum [2–8], such as $\Lambda_c(2286)^+$, $\Lambda_c(2595)^+$, $\Lambda_c(2625)^+$, $\Lambda_c(2760)^+$, $\Lambda_c(2860)^+$, $\Lambda_c(2880)^+$, $\Sigma_c(2455)^{0,+,++}$, $\Sigma_c(2520)^{0,+,++}$, $\Sigma_c(2880)^{0,+,++}$, and so on. The advanced experimental progress has motivated theorists to explore their properties in many theoretical methods [9–15]. We believe the studies of the charmed baryons can deepen our understanding of the

nonperturbative behavior of the QCD in the low-energy regions.

Months ago, the Belle Collaboration reported a new structure called $\Lambda_c(2910)^+$, via the $\bar{B}^0 \to \Sigma_c(2455)\pi\bar{p}$ decay process [16]. Its mass and width are measured to be $2913.8 \pm 5.6 \pm 3.8$ MeV and $51.8 \pm 20.0 \pm 18.8$ MeV, respectively. In fact, the observed $\Lambda_c(2910)^+$ is a continuation of the experimental studies of Λ_c baryons in the past. In 2006, the *BABAR* Collaboration released the observation of $\Lambda_c(2940)^+$ in the $D^0 p$ invariant mass spectrum [17]. Later, Belle confirmed $\Lambda_c(2940)^+$ in the decay mode $\Lambda_c(2940)^+ \to \Sigma_c(2455)^{0,++}\pi^{+,-}$ [18]. In 2017, the LHCb Collaboration also observed it [19] and preferred its possible assignment with $J^P = 3/2^-$. Till now, the Particle Data Group [1] has listed its mass and width as $M = 2939.6^{+1.3}_{-1.5}$ MeV and $\Gamma = 20^{+6}_{-5}$ MeV, respectively.

In theory, the newly observed $\Lambda_c(2910)^+$ is studied in several works. $\Lambda_c(2910)^+$ was interpreted as $\Lambda_c(2P, 1/2^-)$ with the QCD sum rule [20]. In Ref. [21], the authors treated $\Lambda_c(2910)^+$ as a good candidate of $\Lambda_c|J^P = 5/2^-, 2\rangle_\rho$ by investigating the strong decay of the low-lying $1P$-wave of the ρ mode excitation; however, the

*[*]liuzhanwei@lzu.edu.cn
[†]luosq15@lzu.edu.cn
[‡]wangfl2016@lzu.edu.cn
[§]wangbo@hbu.edu.cn
[‖]xuh2020@nwnu.edu.cn

$\Lambda_c|J^P = 3/2^-, 2\rangle_\rho$ and $\Lambda_c|J^P = 1/2^-, 1\rangle_\rho$ assignments cannot be excluded. The authors in Ref. [22] arranged the $\Lambda_c(2910)^+$ as the $2P$-wave of the λ mode excitation with $J^P = 1/2^-$ or $3/2^-$ by examining its strong decay.

In the past, the charmed baryons $\Lambda_c(2P, 1/2^-)$ and $\Lambda_c(2P, 3/2^-)$ have already been studied in the quenched quark model [2–8], while the strong decays of $\Lambda_c(2P, 1/2^-)$ and $\Lambda_c(2P, 3/2^-)$ were also studied in Refs. [22–28]. It is hard to explain $\Lambda_c(2940)^+$ with simple bare udc structure because its experimental mass is usually about 100 MeV smaller than the theoretical expectations [2–4]. Thus, it has stimulated great interest of theorists in studying the inner structure of $\Lambda_c(2940)^+$.

An important fact is that $\Lambda_c(2940)^+$ is located below the D^*N threshold about 6 MeV, so several theoretical groups treat $\Lambda_c(2940)^+$ as a D^*N molecular state [29–38]. For example, within the one-boson-exchange model, $\Lambda_c(2940)^+$ was treated as the D^*N molecular state with $I(J^P) = 0(1/2^+)$ or $0(3/2^-)$ [39]. The D^*N bound state was also found in the $[D^*N]^{I=3/2}_{J=3/2}$ channel within other models, such as the QCD sum rule, constituent quark model, and chiral quark model [40–43]. In Refs. [44,45], the chiral effective field theory was applied to the D^*N interaction, and two bound solutions were found with a little mass gap for the isospin $I = 0$ channels, which shows the $\Lambda_c(2940)^+$ could be either $[D^*N]^{I=0}_{J=1/2}$ or $[D^*N]^{I=0}_{J=3/2}$. Thus, the interaction between D^*N plays a key role in forming this physical state.

Therefore, we conclude that the bare triquark states and the D^*N channel should be equally important for $\Lambda_c(2940)^+$ and $\Lambda_c(2910)^+$. Under an unquenched quark model, the authors in Ref. [46] study $\Lambda_c(2P, 1/2^-)$ and $\Lambda_c(2P, 3/2^-)$ considering the coupling to the D^*N channel. They conclude that the mass in spin $1/2$ becomes larger than that in spin $3/2$ in the unquenched picture, so that the mass relation is reversed compared to the quenched picture (see Fig. 1).
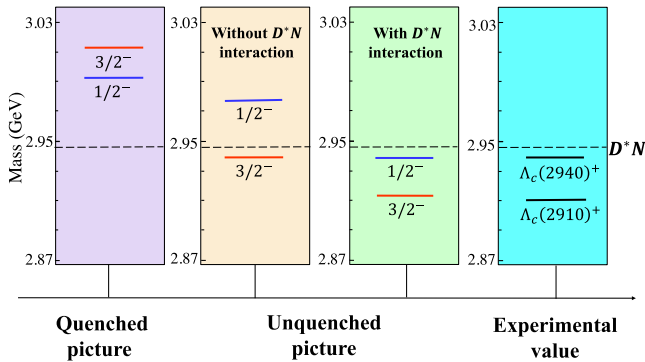

FIG. 1. The masses comparison between the undressed conventional baryons [46], the conventional baryons dressed by D^*N without considering D^*N interaction [46], the dressed states with the D^*N interaction in this work, and the experimental baryons [1,16–19].

The coupled-channel effects among a bare triquark state and hadron-hadron channels are widely studied in the case of $\Lambda(1405)^0$, $D^*_{s0}(2317)^\pm$, $D^*_{s1}(2460)^\pm$, $X(3872)$, etc. [47–61]. In Refs. [57,62–64], they studied the structure of $X(3872)$ with coupled $D\bar{D}^*$ channel and obtained it as a mixture of bare $c\bar{c}$ core and $D\bar{D}^*$ component. Moreover, in Refs. [65–68], the $D^*_{s0}(2317)^\pm$ and $D^*_{s1}(2460)^\pm$ were also studied by the unquenched quark model, and their structure information was revealed as the mixture of bare $c\bar{s}$ cores and $D^{(*)}K$ component. In addition, taking into account the S-wave $D^{(*)}K$ interaction, the authors in Ref. [69] studied the D_s states under the Hamiltonian effective field theory and found the $D^{(*)}K$ interaction can cause significant mass shifts and lower the mass. According to their investigation, we think including the hadron-hadron interaction is important in the coupled-channel studies.

In the present work, we try to interpret $\Lambda_c(2910)^+$ and $\Lambda_c(2940)^+$ at the same time within a consistent framework with the coupled-channel effects between the bare triquark states and the D^*N channel, as well as the D^*N-D^*N interactions. The physical states $\Lambda_c(2910)^+$ and $\Lambda_c(2940)^+$ can be produced as a competition between the bare $2P$-wave udc cores and S-wave D^*N components. We believe our effort can lead us to disclose the true natures of $\Lambda_c(2910)^+$ and $\Lambda_c(2940)^+$.

This article is organized as follows. After the Introduction, we present the details of the theoretical framework in Sec. II, which includes the full Hamiltonian and coupled-channel equation involving the interaction of the hadron-hadron channel. The detailed interactions will be given in Sec. III within the chiral effective field theory and quark-pair-creation model. In Sec. IV, we present our numerical results and discussion. A short summary follows in Sec. V.

II. FRAMEWORK

If we consider the mixing between the bare state $|\Psi_0\rangle$ and $|BC, \mathbf{p}\rangle$ channel, the physical state [64,70–80] can be represented by

$$|\Psi\rangle = c_0|\Psi_0\rangle + \int d^3\mathbf{p}\chi_{BC}(\mathbf{p})|BC, \mathbf{p}\rangle. \quad (2.1)$$

Here, c_0 is the possible amplitude to discover the bare state $|\Psi_0\rangle$ in the physical state $|\Psi\rangle$, $\chi_{BC}(\mathbf{p})$ denotes the relative wave function in the hadron-hadron channel $|BC, \mathbf{p}\rangle$, and the normalizing condition is given by

$$|c_0|^2 + \int |\chi_{BC}(\mathbf{p})|^2 d^3\mathbf{p} = 1. \quad (2.2)$$

Then, the full coupled-channel equation can be formally expressed as

$$\begin{pmatrix} \hat{H}_0 & \hat{H}_I \\ \hat{H}_I & \hat{H}_{BC} \end{pmatrix} \begin{pmatrix} c_0|\Psi_0\rangle \\ \chi_{BC}(\mathbf{p})|BC,\mathbf{p}\rangle \end{pmatrix} = M \begin{pmatrix} c_0|\Psi_0\rangle \\ \chi_{BC}(\mathbf{p})|BC,\mathbf{p}\rangle \end{pmatrix}.$$

$$(2.3)$$

By expanding Eq. (2.3), one obtains

$$\hat{H}_0 c_0|\Psi_0\rangle + \hat{H}_I \chi_{BC}(\mathbf{p})|BC,\mathbf{p}\rangle = M c_0|\Psi_0\rangle \quad (2.4)$$

and

$$\hat{H}_I c_0|\Psi_0\rangle + \hat{H}_{BC} \chi_{BC}(\mathbf{p})|BC,\mathbf{p}\rangle = M \chi_{BC}(\mathbf{p})|BC,\mathbf{p}\rangle. \quad (2.5)$$

Here, $\hat{H}_0$ only works on the bare state $|\Psi_0\rangle$, i.e.,

$$\hat{H}_0|\Psi_0\rangle = M_0|\Psi_0\rangle, \quad (2.6)$$

where M_0 is the bare mass, which can be well determined by the traditional potential models, such as the nonrelativistic three-quark model [46,81–84], quark-diquark model [2,3,13], Capstick-Isgur model [4], and so on. For the most low-lying singly charmed baryons, these traditional potential models have good predictive powers in studying the mass spectra. $\hat{H}_0$ is usually written as a sum of two parts, i.e.,

$$\hat{H}_0 = \sum_i E_i + \sum_{i,j} V_{ij}, \quad (2.7)$$

where E_i is free energy for ith constituent quark and the V_{ij} is the effective potential between two quarks where the form depends on specific potential models.

In addition, $\hat{H}_I$ in Eq. (2.3) represents the transition Hamiltonian between the bare state and the intermediate BC channel. $\hat{H}_{BC}$ is the Hamiltonian describing BC-BC interaction. With the above definitions, multiplying $\langle\Psi_0|$ on each side in Eq. (2.4), one obtains

$$M_0 c_0 + \int \chi_{BC}(\mathbf{p}) H^*_{\Psi_0 \to BC}(\mathbf{p}) d^3\mathbf{p} = M c_0. \quad (2.8)$$

Then, c_0 can be obtained

$$c_0 = \int \frac{\chi_{BC}(\mathbf{p}) H^*_{\Psi_0 \to BC}(\mathbf{p})}{M - M_0} d^3\mathbf{p}. \quad (2.9)$$

On the other hand, multiplying $\langle BC, \mathbf{p}'|$ on each side of Eq. (2.5), we have

$$c_0 H_{\Psi_0 \to BC}(\mathbf{p}') + \int \langle BC, \mathbf{p}'|\hat{H}_{BC}\chi_{BC}(\mathbf{p})|BC,\mathbf{p}\rangle d^3\mathbf{p}$$
$$= M\chi_{BC}(\mathbf{p}'). \quad (2.10)$$

The $\hat{H}_{BC}$ is the Hamiltonian of the intermediate BC channel, which includes two parts, i.e., the free and inner

interactions. Explicitly, the matrix element sandwiching the $\hat{H}_{BC}$ can be expressed as

$$\int \langle BC, \mathbf{p}'|\hat{H}_{BC}\chi_{BC}(\mathbf{p})|BC,\mathbf{p}\rangle d^3\mathbf{p}$$

$$= \int \langle BC, \mathbf{p}'|E_{BC}(\mathbf{p})\delta^3(\mathbf{p}-\mathbf{p}')\chi_{BC}(\mathbf{p})|BC,\mathbf{p}\rangle d^3\mathbf{p}$$

$$+ \int \langle BC, \mathbf{p}'|V_{BC \to BC}(\mathbf{p},\mathbf{p}')\chi_{BC}(\mathbf{p})|BC,\mathbf{p}\rangle d^3\mathbf{p}$$

$$= E_{BC}(\mathbf{p}')\chi_{BC}(\mathbf{p}') + \int V_{BC \to BC}(\mathbf{p},\mathbf{p}')\chi_{BC}(\mathbf{p}) d^3\mathbf{p}, \quad (2.11)$$

where $E_{BC}(\mathbf{p}') = m_B + m_C + \frac{p'^2}{2m_B} + \frac{p'^2}{2m_C}$ is the free energy of the intermediate BC channel and $V_{BC \to BC}(\mathbf{p},\mathbf{p}')$ is the hadron-hadron interaction in the momentum space. With Eqs. (2.9)–(2.11), we can obtain the following coupled-channel equation:

$$E_{BC}(\mathbf{p}')\chi_{BC}(\mathbf{p}') + H_{\Psi_0 \to BC}(\mathbf{p}') \int \frac{\chi_{BC}(\mathbf{p}) H^*_{\Psi_0 \to BC}(\mathbf{p})}{M - M_0} d^3\mathbf{p}$$

$$+ \int \chi_{BC}(\mathbf{p}) V_{BC \to BC}(\mathbf{p},\mathbf{p}') d^3\mathbf{p} = M\chi_{BC}(\mathbf{p}'). \quad (2.12)$$

It is equivalent to the following expression:

$$\int \left(\frac{H^*_{\Psi_0 \to BC}(\mathbf{p}) H_{\Psi_0 \to BC}(\mathbf{p}')}{M - M_0} + V_{BC \to BC}(\mathbf{p},\mathbf{p}') \right) \chi_{BC}(\mathbf{p}) d^3\mathbf{p}$$

$$+ E_{BC}(\mathbf{p}')\chi_{BC}(\mathbf{p}') = M\chi_{BC}(\mathbf{p}'). \quad (2.13)$$

Thus, the final χ_{BC}-coupled-channel equation (2.13) contains the interaction between hadron B and C. By solving Eq. (2.13), we can get the physical mass that includes the contribution of both the hadron BC channel and the bare state. The two terms inside the parentheses of Eq. (2.13) are responsible for the mass shift.

For obtaining the solution of Eq. (2.13), we use a set of the complete base expansion method, where the complete basis can be chosen as the harmonic oscillator basis, the Gaussian basis, and so on. For example, we use the Gaussian basis to replace the $\chi_{BC}(\mathbf{p})$ in Eq. (2.13) [85,86],

$$\chi_{BC}(\mathbf{p}) = \sum_{i=1}^{N_{\max}} C_{il}\phi^p_{ilm}(\mathbf{p}), \quad (2.14)$$

where C_{il} is the coefficient of the corresponding basis and $\phi^p_{ilm}(\mathbf{p})$ is the Gaussian basis. In the coordinate space,

$$\phi^r_{nlm}(\nu_n, \mathbf{r}) = N_{nl} r^l e^{-\nu_n r^2} Y_{lm}(\hat{\mathbf{r}}), \quad (2.15)$$

where N_{nl} is normalization constant. By the Fourier transform, the Gaussian basis in momentum space can be written as

$$\phi_{nlm}^{p}(\nu_n, \mathbf{p}) = (-i)^l \phi_{nlm}^{r}\left(\frac{1}{4\nu_n}, \mathbf{p}\right). \qquad (2.16)$$

In Eqs. (2.15) and (2.16), v_n is the Gaussian ranges, i.e.,

$$\nu_n = 1/r_n^2, \qquad r_n = r_1 a^{n-1} \quad (n = 1, 2 \ldots N_{\max}). \qquad (2.17)$$

With the above Gaussian basis, all the Hamilton matrix elements can be expressed in simple forms. We define

$$T_{fi} = \int \mathrm{d}^3\mathbf{p}' \phi_{flm}^{p*}(\nu_f, \mathbf{p}') E_{BC}(\mathbf{p}') \phi_{ilm}^{p}(\nu_i, \mathbf{p}'),$$

$$\mathcal{M}_{fi} = \int \mathrm{d}^3\mathbf{p}' \mathrm{d}^3\mathbf{p} \frac{H_{\Psi_0 \to BC}^{*}(\mathbf{p}) H_{\Psi_0 \to BC}(\mathbf{p}')}{M - M_0}$$
$$\times \phi_{flm}^{p*}(\nu_f, \mathbf{p}') \phi_{ilm}^{p}(\nu_i, \mathbf{p}),$$

$$V_{fi} = \int \mathrm{d}^3\mathbf{p}' \mathrm{d}^3\mathbf{p} \phi_{flm}^{p*}(\nu_f, \mathbf{p}') V_{BC \to BC}(\mathbf{p}, \mathbf{p}') \phi_{ilm}^{p}(\nu_i, \mathbf{p}),$$

$$N_{if} = \int \mathrm{d}^3\mathbf{r}' \phi_{flm}^{r*}(\nu_f, \mathbf{r}') \phi_{ilm}^{r}(\nu_i, \mathbf{r}'). \qquad (2.18)$$

With the above matrix elements, Eq. (2.13) is equivalent to following general eigenvalue equation

$$\sum_{i=1}^{N_{\max}} C_{il}(T_{fi} + \mathcal{M}_{fi} + V_{fi}) = M \sum_{i=1}^{N_{\max}} C_{il} N_{fi}. \qquad (2.19)$$

Here, the coefficient C_{il} can be solved by the Rayleigh-Ritz variational principle. Because both sides of Eq. (2.19) depend on M, we are dealing with a special eigenvalue equation. First, we replace M with M_E on the right side. Then, we scan all possible M on the left side of the new equation in a reasonable range and obtain the eigenvalues M_E. At last, the solution comes as M equals M_E.

If the interaction $V_{BC \to BC}(\mathbf{p}, \mathbf{p}')$ of the direct hadron-hadron channel is neglected, we can extract the approximate mass M,

$$M = M_0 + \int \frac{|H_{A^{\mathrm{bare}} \to BC}(\mathbf{p})|^2}{M - E_{BC}(\mathbf{p})} \mathrm{d}^3\mathbf{p}, \qquad (2.20)$$

and obtain approximate wave function $\chi_{BC}(\mathbf{p})$,

$$\chi_{BC}(\mathbf{p}) = \frac{H_{\Psi_0 \to BC}(\mathbf{p})}{M - E_{BC}(\mathbf{p})} c_0. \qquad (2.21)$$

III. DETAILED INTERACTIONS

In this section, we provide the D^*N interaction in Sec. III A and the coupling between the bare state and the D^*N in Sec. III B. These determine the coupled-channel effects of $\Lambda_c(2940)^+$ and $\Lambda_c(2910)^+$.

A. D^*N interaction

First, we focus on the detailed potential $V_{BC \to BC}$ for the S-wave D^*N interaction, and we employ the chiral effective field theory, which is a powerful instrument to study the hadron-hadron interaction [45,87–95]. In the heavy-flavor hadron systems, the application of the chiral effective field theory has led to some achievements for predicting the bound states of $\bar{B}^{(*)}\bar{B}^{(*)}$, DD^*, $D\bar{D}^*$, $\Sigma_c\bar{D}^{(*)}$, and so on [45,96–105]. With the experience in these works, the D^*N interaction can also be studied within the chiral effective field theory.

We will investigate four channels in the D^*N system, i.e., isospin $I = 0$, 1 and spin $J = 1/2$, 3/2. Therefore, we consider the following flavor wave functions:

$$|1, 1\rangle = |pD^{*+}\rangle,$$

$$|1, 0\rangle = \frac{1}{\sqrt{2}}(|pD^{*0}\rangle - |nD^{*+}\rangle),$$

$$|1, -1\rangle = |nD^{*0}\rangle,$$

$$|0, 0\rangle = \frac{1}{\sqrt{2}}(|pD^{*0}\rangle + |nD^{*+}\rangle).$$

In the following, we first give the chiral Lagrangians and Feynman diagrams including tree and one-loop diagrams of the D^*N system. Then, we provide the D^*N effective potentials in momentum space at the next-to-leading order $\mathcal{O}(\epsilon^2)$. They include the contact term, one-pion-exchange, and two-pion-exchange contributions, which approximatively correspond to the short-range, long-range, and middle-range interactions, respectively. In addition, we also consider the $\Delta(1232)$ contribution. Through the Fourier transformation, we also obtain the effective potentials in coordinate space.

The leading-order πN Lagrangian [106–108] is given by

$$\mathcal{L}_{\mathcal{N}\varphi} = \bar{\mathcal{N}}(iv \cdot \mathcal{D} + 2g_a \mathcal{S} \cdot u)\mathcal{N}, \qquad (3.1)$$

where $\mathcal{N} = (p, n)^T$ denotes the large component of the nucleon field under the nonrelativistic reduction, $v = (1, 0, 0, 0)$ stands for the 4-velocity of the nucleon, $\mathcal{D}_\mu = \partial_\mu + \Gamma_\mu$ is covariant derivative, g_a is the axial-vector coupling constant, and $\mathcal{S}^\mu = \frac{i}{2}\gamma_5\sigma^{\mu\nu}v_\nu$ denotes the Pauli-Lubanski spin vector. The chiral connection Γ_μ and axial-vector current u_μ are expressed as

$$\Gamma_\mu \equiv \frac{1}{2}[\xi^\dagger, \partial_\mu \xi] \equiv \tau^i \Gamma_\mu^i, \quad u_\mu \equiv \frac{i}{2}\{\xi^\dagger, \partial_\mu \xi\} \equiv \tau^i \omega_\mu^i, \qquad (3.2)$$

where τ^i is a 2-component Pauli matrix in the isospin space, i.e.,

$$\xi^2 = U = \exp\left(\frac{i\phi}{f_\pi}\right), \qquad \phi = \begin{pmatrix} \pi^0 & \sqrt{2}\pi^+ \\ \sqrt{2}\pi^- & -\pi^0 \end{pmatrix}, \quad (3.3)$$

and f_π is the pion decay constant.

The $D^{(*)}\pi$ Lagrangian at the leading order is given by [109–112]

$$\mathcal{L}_{\mathcal{H}\varphi} = i\langle \mathcal{H}v\cdot\mathcal{D}\bar{\mathcal{H}}\rangle - \frac{1}{8}\delta_b\langle\mathcal{H}\sigma^{\mu\nu}\bar{\mathcal{H}}\sigma_{\mu\nu}\rangle + g\langle\mathcal{H}\slashed{u}\gamma_5\bar{\mathcal{H}}\rangle, \quad (3.4)$$

where $\langle\cdots\rangle$ denotes the trace in the spinor space and δ_b is mass shift between D^* and D, i.e., $\delta_b = m_{D^*} - m_D$, and it does not disappear in the chiral limit. g stands for the axial coupling constant. The $\mathcal{H}$ represents the superfield for the charmed mesons, which reads

$$\mathcal{H} = \frac{1+\slashed{v}}{2}(P_\mu^*\gamma^\mu + iP\gamma_5),$$

$$\bar{\mathcal{H}} = \gamma^0 H^\dagger \gamma^0 = (P_\mu^{*\dagger}\gamma^\mu + iP^\dagger\gamma_5)\frac{1+\slashed{v}}{2}, \quad (3.5)$$

with $P = (D^0, D^+)^T$ and $P^* = (D^{*0}, D^{*+})^T$, respectively.

The leading-order contact Lagrangian describes the short distance interaction between the nucleon and charmed meson [44], which can be written as

$$\mathcal{L}_{\mathcal{NH}} = D_a\bar{\mathcal{N}}\mathcal{N}\langle\bar{\mathcal{H}}\mathcal{H}\rangle + D_b\bar{\mathcal{N}}\gamma_\mu\gamma_5\mathcal{N}\langle\bar{\mathcal{H}}\gamma^\mu\gamma_5\mathcal{H}\rangle$$
$$+ E_a\bar{\mathcal{N}}\tau_i\mathcal{N}\langle\bar{\mathcal{H}}\tau_i\mathcal{H}\rangle + E_b\bar{\mathcal{N}}\gamma_\mu\gamma_5\tau_i\mathcal{N}\langle\bar{\mathcal{H}}\gamma^\mu\gamma_5\tau_i\mathcal{H}\rangle, \quad (3.6)$$

where D_a, D_b, E_a, and E_b are four low-energy constants (LECs).

Finally, considering the strong coupling between $\Delta(1232)$ and πN [113–117], the Lagrangian of the Δ-N-π coupling [118] is given by

$$\mathcal{L}_{\Delta\varphi} = -\bar{T}_i^\mu(iv\cdot\mathcal{D}^{ij} - \delta^{ij}\delta_a + 2g_1\mathcal{S}\cdot u^{ij})g_{\mu\nu}\mathcal{T}_j^\nu, \quad (3.7)$$

$$\mathcal{L}_{\Delta\mathcal{N}\varphi} = 2g_\delta(\bar{T}_i^\mu g_{\mu\alpha}\omega_i^\alpha\mathcal{N} + \bar{\mathcal{N}}\omega_i^{\alpha\dagger}g_{\alpha\mu}\mathcal{T}_i^\mu), \quad (3.8)$$

where $\delta_a = m_\Delta - m_N$ and $g_1 = \frac{9}{5}g_a$ [118]. g_δ is the coupling constant for the $\Delta N\pi$ vertex. The matrix form of $\mathcal{T}_i^\mu$ reads

$$\mathcal{T}_\mu^1 = \frac{1}{\sqrt{2}}\begin{pmatrix} \Delta^{++} - \frac{1}{\sqrt{3}}\Delta^0 \\ \frac{1}{\sqrt{3}}\Delta^+ - \Delta^- \end{pmatrix}_\mu,$$

$$\mathcal{T}_\mu^2 = \frac{i}{\sqrt{2}}\begin{pmatrix} \Delta^{++} + \frac{1}{\sqrt{3}}\Delta^0 \\ \frac{1}{\sqrt{3}}\Delta^+ + \Delta^- \end{pmatrix}_\mu,$$

$$\mathcal{T}_\mu^3 = -\sqrt{\frac{2}{3}}\begin{pmatrix} \Delta^+ \\ \Delta^0 \end{pmatrix}_\mu. \quad (3.9)$$

Here, $\mathcal{T}_i^\mu$ denotes the spin-3/2 and isospin-3/2 field $\Delta(1232)$ in the nonrelativistic reduction.

In the framework of the heavy hadron chiral perturbation theory, the scattering amplitudes of the D^*N system can be expanded order by order in powers of a small quantity $\varepsilon = q/\Lambda_\chi \sim 1$ GeV, where q is either the momentum of Goldstone bosons or the residual momentum of heavy flavor hadrons and Λ_χ represents either the chiral breaking scale or the mass of a heavy hadron. The expansion respects the power counting rule [106,107]. The Feynman diagrams of $\mathcal{O}(\epsilon^0)$ contact term, $\mathcal{O}(\epsilon^0)$ one-pion-exchange, and $\mathcal{O}(\epsilon^2)$ two-pion-exchange are illustrated in Fig. 2.

With the chiral Lagrangians and these Feynman diagrams, we can obtain their Feynman amplitudes $\mathcal{M}$. Then, we use the Breit approximation $\mathcal{V} = -\mathcal{M}/(\Pi_i 2m_i\Pi_f 2m_f)^{1/2}$ to relate the scattering amplitude $\mathcal{M}$ to the effective potential $\mathcal{V}$ [44], where m_i and m_f are the masses of the initial and final states, respectively. These effective potentials of the Feynman diagrams in Fig. 2 consist of the following parts:
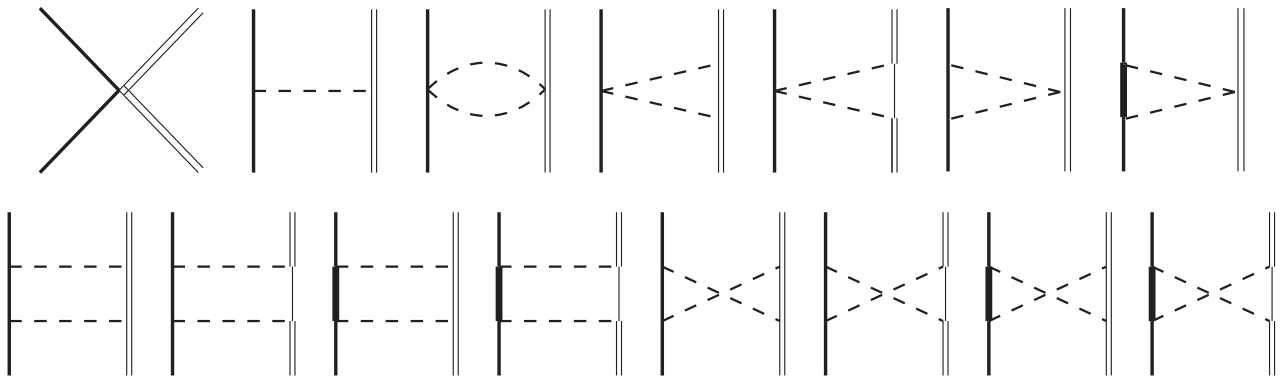

FIG. 2. The Feynman diagrams of contact term at $\mathcal{O}(\epsilon^0)$, one-pion-exchange at $\mathcal{O}(\epsilon^0)$, and two-pion-exchange at $\mathcal{O}(\epsilon^2)$. The thin, double-thin, thick, heavy-thick, and dashed lines denote the D, D^*, N, $\Delta(1232)$, and pion field, respectively.

$$\mathcal{V}_{\text{total}} = \mathcal{V}_{\text{contact}}^{\text{LO}} + \mathcal{V}_{1-\pi}^{\text{LO}} + \mathcal{V}_{2-\pi}^{\text{NLO}}, \qquad (3.10)$$

where $\mathcal{V}_{\text{contact}}^{\text{LO}}$, $\mathcal{V}_{1-\pi}^{\text{LO}}$, and $\mathcal{V}_{2-\pi}^{\text{NLO}}$ denote $\mathcal{O}(\epsilon^0)$ contact term, $\mathcal{O}(\epsilon^0)$ one-pion-exchange, and $\mathcal{O}(\epsilon^2)$ two-pion-exchange potentials, respectively.

The $\mathcal{V}_{2-\pi}^{\text{NLO}}$ is the sum of the football diagram, triangle diagram, box diagram, and crossed box diagram potentials in Fig. 2, i.e., $\mathcal{V}_{2-\pi}^{\text{NLO}} = \mathcal{V}_{\text{football}} + \mathcal{V}_{\text{triangle}} + \mathcal{V}_{\text{box}} + \mathcal{V}_{\text{crossed-box}}$. These two-pion-exchange diagrams need some loop functions J_{ij}^F, J_{ij}^T, J_{ij}^B, and J_{ij}^R, which can be found in Refs. [96–98,102,105]. To obtain the effective potentials, the two-particle-reducible contribution should be subtracted from these crossed box diagrams by the principal value integral method in Appendix B of Ref. [102]. Additionally, the divergent parts in two-pion-exchange diagrams can be absorbed by unrenormalized LECs in Ref. [44]. In this work, all the parameters for the D^*N interaction are from Ref. [44].

In Fig. 3, we give the D^*N effective potential in momentum space, which can help us to understand the D^*N interaction clearer. For the $[D^*N]_{J=1/2}^{I=0}$ channel in Fig. 3(a), the $\mathcal{O}(\epsilon^0)$ one-pion-exchange potential and $\mathcal{O}(\epsilon^2)$ two-pion-exchange potential are both repulsive. But their repulsive interaction is rather weak. The attractive interaction is dominantly provided by the $\mathcal{O}(\epsilon^0)$ contact interaction. In Fig. 3(b), the $\mathcal{O}(\epsilon^0)$ one-pion-exchange potential is attractive, and the $\mathcal{O}(\epsilon^2)$ two-pion-exchange potential is repulsive, but both of them are rather weak. However, the potential of $\mathcal{O}(\epsilon^0)$ contact term has strong attractive interaction. For the $[D^*N]_{J=1/2}^{I=1}$ channel in Fig. 3(c), the potential of $\mathcal{O}(\epsilon^0)$ contact term and $\mathcal{O}(\epsilon^2)$ two-pion-exchange are both repulsive, but the $\mathcal{O}(\epsilon^0)$ one-pion-exchange is attractive. The total potential has rather weak attraction. From Fig. 3(d), the total potential are not attractive enough. Therefore, the two isoscalar channels $I(J^P) = 0(1/2^-)$ and $I(J^P) = 0(3/2^-)$ provide the stronger attractive interaction in momentum space, and
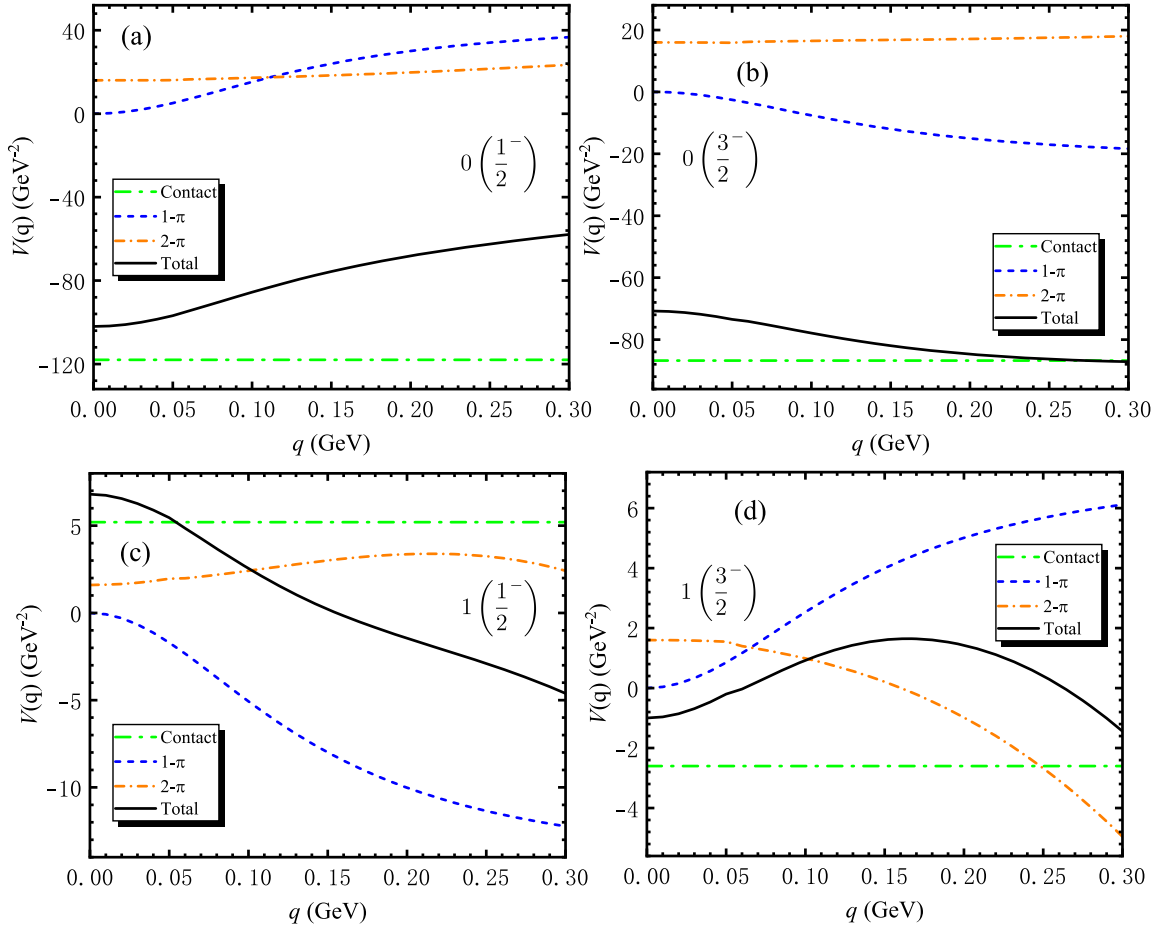

FIG. 3. The D^*N interaction potential in momentum space with the cutoff parameter $\Lambda = 0.4$ GeV, and $q = |\mathbf{q}|$ is the transfer momentum between D^* and N. Here, the green, blue, and red dotted lines describe the contact term potential at $\mathcal{O}(\epsilon^0)$, one-pion-exchange potential at $\mathcal{O}(\epsilon^0)$, and two-pion-exchange potential at $\mathcal{O}(\epsilon^2)$, respectively, while the black solid line denotes the total potential.

we identify the attraction in two $I = 1$ channels is weak. In the following parts, we mainly consider the two isospin $I = 0$ channels. Furthermore, the $\Delta(1232)$ plays a particular role in the D^*N interaction because the coupling between $\Delta(1232)$ and πN system is very strong. The total potential is sensitive to $\Delta(1232)$, which determines its importance in the D^*N interaction.

Based on the obtained effective potential in momentum space $\mathcal{V}(\mathbf{q})$, the effective potential in coordinate space $\mathcal{V}(\mathbf{r})$ can be obtained by the following Fourier transformation:

$$V_{BC \to BC}(\mathbf{r}) = \int \frac{\mathrm{d}^3\mathbf{q}}{(2\pi)^3} e^{i\mathbf{q} \cdot \mathbf{r}} \mathcal{V}(\mathbf{q}) \mathcal{F}(\mathbf{q}). \quad (3.11)$$

Here, $\mathcal{F}(\mathbf{q}) = e^{-\mathbf{q}^{2n}/\Lambda^{2n}}$ is the form factor with Gauss form to suppress the high momentum and renormalize the potential [44,97].

When we employ the chiral effective field theory and use some approximation, such as the transferred energy q^0 between D^* and N, and the residual energies of N and D^* are all set to zero, then the effective potential of D^*N will have the simple form of $V_{BC \to BC}(\mathbf{p}' - \mathbf{p})$. Thus, the $V_{BC \to BC}(\mathbf{p}', \mathbf{p})$ in Eq. (2.11) can be defined as

$$V_{BC \to BC}(\mathbf{p}', \mathbf{p}) = \frac{1}{(2\pi)^3} \int V_{BC \to BC}(\mathbf{r}) e^{i(\mathbf{p}' - \mathbf{p}) \cdot \mathbf{r}} \mathrm{d}^3\mathbf{r}.$$

In this scheme, the matrix element V_{fi} in Eq. (2.18) can be conveniently calculated by

$$V_{fi} = \int \mathrm{d}^3\mathbf{r} \phi_{flm}^{r*}(\nu_f, \mathbf{r}) V_{BC \to BC}(\mathbf{r}) \phi_{ilm}^r(\nu_i, \mathbf{r}). \quad (3.12)$$

B. Interaction between the bare state and D^*N channel

For the interaction Hamiltonian $\hat{H}_I$ between the bare state and D^*N in Eq. (2.3), we employ the quark-pair-creation model [119,120], which has the expression

$$\hat{H}_I = g \int \mathrm{d}^3x \bar{\psi}(x) \psi(x). \quad (3.13)$$

Here, $g = 2m_q \gamma$, m_q is the mass of the creation quark, and the dimensionless parameter γ describes the strength of the quark and antiquark pair creation from the vacuum, which can be determined phenomenologically by the Okubo-Zweig-Iizuka (OZI) allowed decay widths of charmonia.

In the nonrelativistic limit, $\hat{H}_I$ is equivalent to [13]

$$\hat{H}_I = -3\gamma \sum_m \langle 1, m; 1, -m|0, 0\rangle \int \mathrm{d}^3\mathbf{p}_\mu \mathrm{d}^3\mathbf{p}_\nu \delta(\mathbf{p}_\mu + \mathbf{p}_\nu)$$

$$\times \mathcal{Y}_1^m \left(\frac{\mathbf{p}_\mu - \mathbf{p}_\nu}{2}\right) \omega^{(\mu,\nu)} \phi^{(\mu,\nu)} \chi_{-m}^{(\mu,\nu)} b_\mu^\dagger(\mathbf{p}_\mu) d_\nu^\dagger(\mathbf{p}_\nu). \quad (3.14)$$

TABLE I. The mass of bare udc core in $\Lambda_c(2P, 1/2^-)$ and $\Lambda_c(2P, 3/2^-)$ in the different potential models. The masses are in units of MeV.

$J^P(nL)$	Ref. [3]	Ref. [13]	Ref. [2]	Ref. [46]	Ref. [4]
$1/2^-(2P)$	2989	2980	2983	2996	3030
$3/2^-(2P)$	3000	3004	3005	3012	3035

Here, ω, ϕ, χ, and $\mathcal{Y}_1^m$ describe the color, flavor, spin, and orbital angular momentum functions of the quark pair, respectively. $b_\mu^\dagger$ and $d_\nu^\dagger$ are quark and antiquark creation operators, respectively. In this work, we fit the dimensionless parameter γ as 9.45 from the total decay width of $\Sigma_c(2520)$ [1].

The masses of bare $\Lambda_c(2P, 1/2^-)$ and $\Lambda_c(2P, 3/2^-)$ can be obtained by the traditional quark potential models combined with the Gaussian expansion method by solving Eqs. (2.6) and (2.7). In this work, we use different bare masses as input and collect them in Table I. In addition, $H_{\Psi_0 \to BC}^*(\mathbf{p})$ in Eq. (2.13) can be obtained by calculating the transition amplitude $H_{\Lambda_c^{bare}(2P,1/2^-) \to D^*N}(\mathbf{p}) = \langle D^*N, \mathbf{p}|\hat{H}_I|\Lambda_c^{bare}(2P, 1/2^-)\rangle$ and $H_{\Lambda_c^{bare}(2P,3/2^-) \to D^*N}(\mathbf{p}) = \langle D^*N, \mathbf{p}|\hat{H}_I|\Lambda_c^{bare}(2P, 3/2^-)\rangle$ with the quark-pair-creation model.

IV. RESULTS AND DISCUSSIONS

Using the formalism described in Sec. II and the detailed interaction in Sec. III, we can now study the dynamical coupling between the S-wave D^*N channel and bare charmed baryon core $\Lambda_c(2P)$. In the quenched quark model, the charmed baryons are simply treated as the three-quark udc baryons [2–4,13,46]. In the unquenched picture, the physical states $\Lambda_c(2940)^+$ and $\Lambda_c(2910)^+$ consist of both udc core and the S-wave D^*N component. In the former works, the authors of Ref. [46] considered the coupling between udc and D^*N but did not involve the D^*N interaction, while this work contains them both. We list the results of the three approaches in Table II.

From the left column in Table II, the masses of the $\Lambda_c(2P, 1/2^-)$ and $\Lambda_c(2P, 3/2^-)$ from quenched quark model are much larger than those of $\Lambda_c(2940)^+$ and $\Lambda_c(2910)^+$. From the middle columns in Table II, the theoretical masses decrease due to the coupling between the udc core and D^*N, but neither can reach the mass of lower state $\Lambda_c(2910)^+$ [46]. Among them, we can see the coupled-channel effects between the $\Lambda_c(2P, 1/2^-)$ and S-wave $[D^*N]_{J=1/2}^{I=0}$ channel are relatively weak, and thus the mass is only suppressed by about 20 MeV and is still above the D^*N threshold. Neither $\Lambda_c(2940)^+$ nor $\Lambda_c(2910)^+$ can match to it. Meanwhile, the coupled effects between the $\Lambda_c(2P, 3/2^-)$ and S-wave $[D^*N]_{J=3/2}^{I=0}$ channel is strong, and the mass decreases by about 70 MeV and is located below the D^*N threshold.

TABLE II. Comparison among the results from quenched quark model [2–4,13,46], unquenched picture without D^*N interaction [46], and unquenched picture with D^*N interaction in this work. Here, r_{RMS} refers to the root-mean-square radius of the D^*N component, and $P(udc) = c_0^2$ represents the probability of bare udc core in the bound state.

Cases	Quenched picture		Unquenched picture without D^*N interaction			Unquenched picture with D^*N interaction		
J^P	M_0 (MeV)		M (MeV)	r_{RMS} (fm)	$P(udc)$ (%)	M (MeV)	r_{RMS} (fm)	$P(udc)$ (%)
$1/2^-$	Ref. [3]	2989	2974	✗	✗	2936	1.93	16.2
$3/2^-$		3000	2933	1.67	39.7	2908	1.31	29.4
$1/2^-$	Ref. [13]	2980	2955	✗	✗	2934	1.83	21.9
$3/2^-$		3004	2935	1.74	37.0	2909	1.31	27.9
$1/2^-$	Ref. [2]	2983	2962	✗	✗	2935	1.87	19.8
$3/2^-$		3005	2935	1.76	36.3	2909	1.32	27.5
$1/2^-$	Ref. [46]	2996	2985	✗	✗	2937	2.00	13.4
$3/2^-$		3012	2937	1.95	31.4	2911	1.33	25.2
$1/2^-$	Ref. [4]	3030	3036	✗	✗	2940	2.32	5.08
$3/2^-$		3035	2943	2.93	15.8	2916	1.38	18.7

From the right columns in Table II, the D^*N interaction further lowers the theoretical masses of the $\Lambda_c(2P, 1/2^-)$ and $\Lambda_c(2P, 3/2^-)$, which now become very close to those of $\Lambda_c(2940)^+$ and $\Lambda_c(2910)^+$, respectively. Thus, we assign $\Lambda_c(2910)^+$ with $J^P = 3/2^-$ and $\Lambda_c(2940)^+$ with $J^P = 1/2^-$. As we can see, the attractive D^*N interaction plays a crucial role in reproducing the experimental $\Lambda_c(2940)^+$ and $\Lambda_c(2910)^+$.

In the unquenched pictures with or without D^*N interaction, the mass for $J^P = 1/2^-$ is larger than that for $3/2^-$, which is different from the quenched case. Such a mass-inversion phenomenon also happens in the $N(1535)$-$N(1440)$ case [58,59]. The mass-inversion phenomenon comes from the two factors in this work: 1) under the chiral effective field theory [44], the energy level in S-wave $[D^*N]^{I=0}_{J=1/2}$ channel is larger than that in the $[D^*N]^{I=0}_{J=3/2}$ channel, and 2) the coupling between $\Lambda_c(2P, 3/2^-)$ and $[D^*N]^{I=0}_{J=3/2}$ is stronger than that between $\Lambda_c(2P, 1/2^-)$ and $[D^*N]^{I=0}_{J=1/2}$ [46]. These lead to the mass inversion between $\Lambda_c(2P, 1/2^-)$ and $\Lambda_c(2P, 3/2^-)$.

In Fig. 4, we present the physical mass M dependence on the bare mass M_0 in $\Lambda_c(2P, 1/2^-)$ and $\Lambda_c(2P, 3/2^-)$. One can notice that the physical masses increase as the bare masses. There are differences between the vertical axis and horizontal axis values of points in the curves, which shows that the bare udc core has a significant mass shift due to the effects of S-wave D^*N channel.

By solving Eq. (2.13), one can obtain the radial wave function of D^*N channel and the probability amplitude of bare udc core, which can help us to reveal the role of D^*N channel and bare udc core in the physical state $\Lambda_c(2940)^+$ and $\Lambda_c(2910)^+$. In Table II, we also provide the root-mean-square radius of D^*N component and the probability of bare udc core in the bound state, and we can see the $3/2^-$ state is a little thinner and contains more bare udc core than the $1/2^-$ one.

If neglecting the triquark core, the pure D^*N can also form bound states with masses around 2940 MeV with $J^P = 1/2^-$ and $3/2^-$ [44]. But such assumptions make it difficult to place the bare $2P$ udc states. In Fig. 5, we present the D^*N radial wave functions for the three
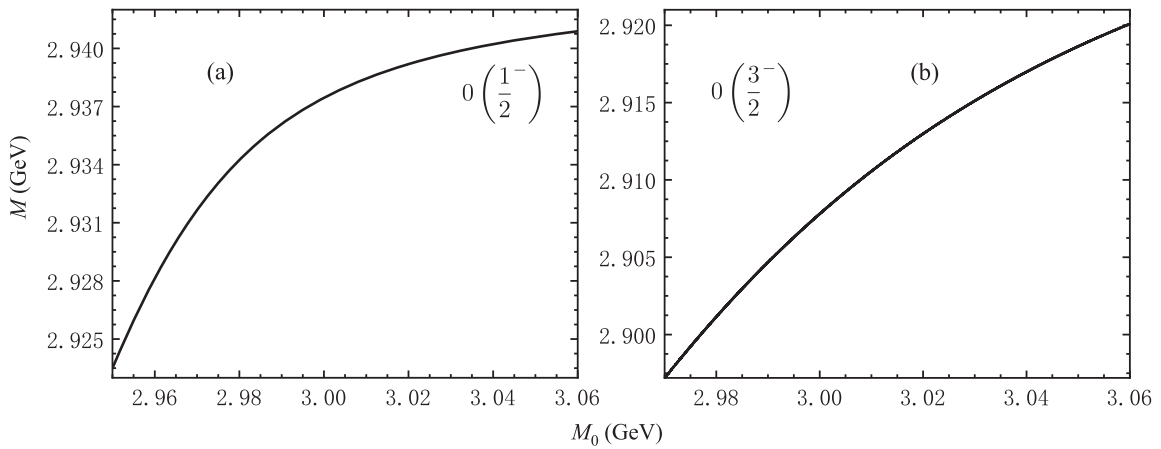

FIG. 4. The physical mass M dependence on the bare mass M_0 in $\Lambda_c(2P, 1/2^-)$ and $\Lambda_c(2P, 3/2^-)$, respectively.
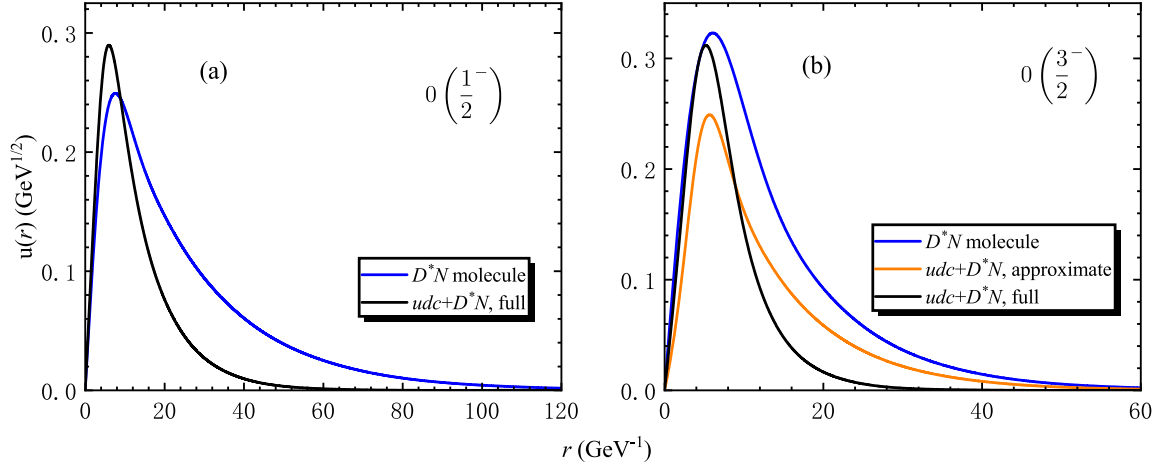
FIG. 5. The D^*N radial wave functions for the pure D^*N molecule ('D^*N molecule'), udc core dressed by D^*N without considering D^*N interaction ('$udc + D^*N$, approximate'), and the dressed state with D^*N interaction ('$udc + D^*N$, full'). Here, the cutoff parameter $\Lambda = 0.4$ GeV and the bare masses are adopted from Ref. [46].

circumstances: the pure D^*N molecule, the udc core dressed by D^*N without considering D^*N interaction, and the dressed state with D^*N interaction. From Fig. 5, we can find that the existence of the bare state can make the D^*N bind more tightly. These wave functions can be used to analyze other properties of charmed baryons, and it can help us to distinguish which model is better in future.

As mentioned earlier, the $\Delta(1232)$ plays an important role in these two physical states. If ignoring the contribution of $\Delta(1232)$, the two-pion-exchange potential becomes smaller. We list the results in Table III if turning off $\Delta(1232)$. From the table, the masses of dressed states decrease by about 10 MeV. In two isoscalar states $[D^*N]^{I=0}_{J=1/2}$ and $[D^*N]^{I=0}_{J=3/2}$, the total potentials become more attractive, which bring these two states thinner.

How to get rid of the cutoff dependence in nonperturbative calculations is still an outstanding problem both in hadron physics and nuclear physics. To investigate the cutoff dependence of our results, we list the charmed baryon masses with two different cutoffs in Table IV. One can see that the unquenched masses all become lower with the cutoff becomes larger, and the results at $\Lambda = 0.4$ GeV are more in line with the experimental data. Currently, we can only provide reasonable results in a very narrow range of cutoff due to the restriction of the validity region of the chiral effective field theory.

Moreover, $\Lambda_c(2910)^+$ and $\Lambda_c(2940)^+$ have small decay widths [1,16–19]. In our unquenched calculation, the

$\Lambda_c(2910)^+$ and $\Lambda_c(2940)^+$ lie below the D^*N threshold (see Fig. 1). Thus, the decays to D^*N channel are kinematically forbidden, which may result in small decay widths of these two states. The strong decay widths of $\Lambda_c(2P, 1/2^-)$ and $\Lambda_c(2P, 3/2^-)$ have been studied in Ref. [22], and the results are consistent with our assignment, i.e., $\Lambda_c(2910)^+$ with spin 3/2 and $\Lambda_c(2940)^+$ with spin 1/2.

In our calculation, we gave the possible interpretation that the J^P for $\Lambda_c(2940)$ is $1/2^-$, which is in clear conflict with the preferred $3/2^-$ assignment from the LHCb experiment [19]. However, our results cannot be completely ruled out by the current experiment, and some other articles also agree with the $J^P = 1/2^-$ assignment [2,7,29,34,37,38,44]. Moreover, the LHCb Collaboration concludes that the other solutions with spins 1/2 to 7/2 cannot be excluded [19].

The D^0p mass region in the amplitude fit is 2.8–3.0 GeV in Ref. [19], but only $\Lambda_c(2940)$ was included. Two resonances $\Lambda_c(2940)$ and $\Lambda_c(2910)$ should be taken into account at the same time, and the conclusion may be changed from the new fit in experiment. The J^P assignment for $\Lambda_c(2940)$ should further be measured the other way like the partial wave analysis. Our results should also be further checked by analyzing their other properties in theory.

TABLE III. The results with $\Delta(1232)$ turned off.

J^P (MeV)	M_0 (MeV)	M (MeV)	$r_{\rm RMS}$ (fm)	$P(udc)$ (%)
$1/2^-$	2996	2930	1.67	12.7
$3/2^-$	3012	2902	1.26	22.4

TABLE IV. The cutoff dependence of the charmed baryon masses in units of MeV. The quenched masses are taken from Ref. [46].

J^P	$\Lambda = 0.4$ GeV	$\Lambda = 0.6$ GeV
$1/2^-$	2937	2924
$3/2^-$	2911	2869

V. SUMMARY

With the accumulation of experimental data, a series of charmed baryons has been reported in the past decades. However, some cannot be fitted into the charmed baryon family very well. Inspired by the reported $\Lambda_c(2910)^+$ and $\Lambda_c(2940)^+$ [1,16–19], we use an unquenched picture to study them by considering S-wave D^*N channel coupled with the bare udc core ($\Lambda_c(2P)$), which gives a unified description of $\Lambda_c(2910)^+$ and $\Lambda_c(2940)^+$.

We take into account two important factors in this work, i.e., the D^*N interaction and the triquark-D^*N coupling. In our unquenched picture, we reproduce the masses of $\Lambda_c(2910)^+$ and $\Lambda_c(2940)^+$ and assign $\Lambda_c(2910)^+$ to $J^P = 3/2^-$ and $\Lambda_c(2940)^+$ to $1/2^-$. The results show the unquenched effects lead to the mass inversion phenomenon in the two states, and the D^*N channel is important.

In the present work, we find the D^*N interaction is crucial in forming the physical states. Let us look at Fig. 1 again. There are large gaps between the quenched quark model results and the experimental masses. The $3/2^-$ mass is pulled down more than the $1/2^-$ one by the coupling between the triquark core and the D^*N, which causes the mass inversion phenomenon. The mass spectrum moves down farther after considering the attractive D^*N interaction and is eventually consistent with the experiments.

From our obtained results, we see $\Lambda_c(2910)^+$ and $\Lambda_c(2940)^+$ contain a significant D^*N component, and the bare state can cause the D^*N to bind more compactly. In addition, we also study the influence of $\Delta(1232)$ in the D^*N interaction. If neglecting $\Delta(1232)$, the dressed masses would be about 10 MeV smaller than before.

Revealing the mixed structure of $\Lambda_c(2910)^+$ and $\Lambda_c(2940)^+$ in the unquenched picture, we expect it can be further verified by other theoretical approaches like lattice QCD simulations. In addition to mass, other properties of these two states should also be analyzed within this picture in the future. More importantly, we strongly suggest an experiment to give a further study in the future, which can provide more hints to uncover the nature of $\Lambda_c(2910)^+$ and $\Lambda_c(2940)^+$.

[1] R. L. Workman *et al.* (Particle Data Group), Review of particle physics, Prog. Theor. Exp. Phys. **2022**, 083C01 (2022).

[2] D. Ebert, R. N. Faustov, and V. O. Galkin, Spectroscopy and Regge trajectories of heavy baryons in the relativistic quark-diquark picture, Phys. Rev. D **84**, 014025 (2011).

[3] B. Chen, K. W. Wei, and A. Zhang, Assignments of Λ_Q and Ξ_Q baryons in the heavy quark-light diquark picture, Eur. Phys. J. A **51**, 82 (2015).

[4] S. Capstick and N. Isgur, Baryons in a relativized quark model with chromodynamics, Phys. Rev. D **34**, 2809 (1986).

[5] H. Y. Cheng, Charmed baryon physics circa 2021, Chin. J. Phys. (Taipei) **78**, 324 (2022).

[6] H. Garcilazo, J. Vijande, and A. Valcarce, Faddeev study of heavy baryon spectroscopy, J. Phys. G **34**, 961 (2007).

[7] G. L. Yu, Z. Y. Li, Z. G. Wang, J. Lu, and M. Yan, Systematic analysis of single heavy baryons Λ_Q, Σ_Q and Ω_Q, arXiv:2206.08128.

[8] Y. Kim, Y. R. Liu, M. Oka, and K. Suzuki, Heavy baryon spectrum with chiral multiplets of scalar and vector diquarks, Phys. Rev. D **104**, 054012 (2021).

[9] H. X. Chen, W. Chen, X. Liu, Y. R. Liu, and S. L. Zhu, A review of the open charm and open bottom systems, Rep. Prog. Phys. **80**, 076201 (2017).

[10] V. Crede and W. Roberts, Progress towards understanding baryon resonances, Rep. Prog. Phys. **76**, 076301 (2013).

[11] H. X. Chen, W. Chen, X. Liu, Y. R. Liu, and S. L. Zhu, An updated review of the new hadron states, Rep. Prog. Phys. **86**, 026201 (2023).

[12] Y. Kato and T. Iijima, Open charm hadron spectroscopy at B-factories, Prog. Part. Nucl. Phys. **105**, 61 (2019).

[13] B. Chen, K. W. Wei, X. Liu, and T. Matsuki, Low-lying charmed and charmed-strange baryon states, Eur. Phys. J. C **77**, 154 (2017).

[14] H. X. Chen, W. Chen, X. Liu, and S. L. Zhu, The hidden-charm pentaquark and tetraquark states, Phys. Rep. **639**, 1 (2016).

[15] Y. R. Liu, H. X. Chen, W. Chen, X. Liu, and S. L. Zhu, Pentaquark and Tetraquark states, Prog. Part. Nucl. Phys. **107**, 237 (2019).

[16] Belle Collaboration, Evidence of a New Excited Charmed Baryon Decaying to $\Sigma_c(2455)^{0,++}\pi^{\pm}$, Phys. Rev. Lett. **130**, 031901 (2023).

[17] B. Aubert *et al.* (*BABAR* Collaboration), Observation of a Charmed Baryon Decaying to $D^0 p$ at a Mass near 2.94 GeV/c^2, Phys. Rev. Lett. **98**, 012001 (2007).

[18] K. Abe *et al.* (Belle Collaboration), Experimental Constraints on the Possible J^P Quantum Numbers of the $\Lambda_c(2880)^+$, Phys. Rev. Lett. **98**, 262001 (2007).

[19] R. Aaij *et al.* (LHCb Collaboration), Study of the $D^0 p$ amplitude in $\Lambda_b^0 \to D^0 p \pi^-$ decays, J. High Energy Phys. 05 (2017) 030.

[20] K. Azizi, Y. Sarac, and H. Sundu, Interpretation of the $\Lambda_c(2910)^+$ baryon newly seen by Belle Collaboration and its possible bottom partner, Eur. Phys. J. C **82**, 920 (2022).

[21] W. J. Wang, L. Y. Xiao, and X. H. Zhong, Strong decays of the low-lying ρ-mode 1P-wave singly heavy baryons, Phys. Rev. D **106**, 074020 (2022).

[22] Q. F. Lü, L. Y. Xiao, Z. Y. Wang, and X. H. Zhong, Strong decay of $\Lambda_c(2940)$ as a 2P state in the Λ_c family, Eur. Phys. J. C **78**, 599 (2018).

[23] C. Chen, X. L. Chen, X. Liu, W. Z. Deng, and S. L. Zhu, Strong decays of charmed baryons, Phys. Rev. D **75**, 094017 (2007).

[24] X. H. Zhong and Q. Zhao, Charmed baryon strong decays in a chiral quark model, Phys. Rev. D **77**, 074008 (2008).

[25] J. He, Z. Ouyang, X. Liu, and X. Q. Li, Production of charmed baryon $\Lambda_c(2940)^+$ at PANDA, Phys. Rev. D **84**, 114010 (2011).

[26] Q. F. Lü and X. H. Zhong, Strong decays of the higher excited Λ_Q and Σ_Q baryons, Phys. Rev. D **101**, 014017 (2020).

[27] J. J. Guo, P. Yang, and A. Zhang, Strong decays of observed Λ_c baryons in the $^3P_0$ model, Phys. Rev. D **100**, 014001 (2019).

[28] K. Gong, H. Y. Jing, and A. Zhang, Possible assignments of highly excited $\Lambda_c(2860)^+$, $\Lambda_c(2880)^+$ and $\Lambda_c(2940)^+$, Eur. Phys. J. C **81**, 467 (2021).

[29] X. G. He, X. Q. Li, X. Liu, and X. Q. Zeng, $\Lambda_c(2940)^+$: A possible molecular state?, Eur. Phys. J. C **51**, 883 (2007).

[30] H. Y. Cheng and C. K. Chua, Strong decays of charmed baryons in heavy hadron chiral perturbation theory, Phys. Rev. D **75**, 014006 (2007).

[31] Y. Dong, A. Faessler, T. Gutsche, and V. E. Lyubovitskij, Strong two-body decays of the $\Lambda_c(2940)^+$ in a hadronic molecule picture, Phys. Rev. D **81**, 014006 (2010).

[32] Y. Dong, A. Faessler, T. Gutsche, S. Kumano, and V. E. Lyubovitskij, Radiative decay of $\Lambda_c(2940)^+$ in a hadronic molecule picture, Phys. Rev. D **82**, 034035 (2010).

[33] Y. Dong, A. Faessler, T. Gutsche, S. Kumano, and V. E. Lyubovitskij, Strong three-body decays of $\Lambda_c(2940)^+$, Phys. Rev. D **83**, 094005 (2011).

[34] X. Y. Wang, A. Guskov, and X. R. Chen, $\Lambda_c^*(2940)^+$ photoproduction off the neutron, Phys. Rev. D **92**, 094032 (2015).

[35] O. Romanets, L. Tolos, C. Garcia-Recio, J. Nieves, L. L. Salcedo, and R. G. E. Timmermans, Charmed and strange baryon resonances with heavy-quark spin symmetry, Phys. Rev. D **85**, 114032 (2012).

[36] H. Y. Cheng and C. K. Chua, Strong decays of charmed baryons in heavy hadron chiral perturbation theory: An update, Phys. Rev. D **92**, 074014 (2015).

[37] J. J. Xie, Y. B. Dong, and X. Cao, Role of the $\Lambda_c^+(2940)$ in the $\pi^- p \to D^- D^0 p$ reaction close to threshold, Phys. Rev. D **92**, 034029 (2015).

[38] Y. Huang, J. He, J. J. Xie, and L. S. Geng, Production of the $\Lambda_c(2940)$ by kaon-induced reactions on a proton target, Phys. Rev. D **99**, 014045 (2019).

[39] J. He, Y. T. Ye, Z. F. Sun, and X. Liu, The observed charmed hadron $\Lambda_c(2940)^+$ and the D^*N interaction, Phys. Rev. D **82**, 114029 (2010).

[40] P. G. Ortega, D. R. Entem, and F. Fernandez, Quark model description of the $\Lambda_c(2940)^+$ as a molecular D^*N state and the possible existence of the $\Lambda_b(6248)$, Phys. Lett. B **718**, 1381 (2013).

[41] P. G. Ortega, D. R. Entem, and F. Fernández, Hadronic molecules in the open charm and open bottom baryon spectrum, Phys. Rev. D **90**, 114013 (2014).

[42] J. R. Zhang, Possibility of $\Sigma_c(2800)$ and $\Lambda_c(2940)^+$ as S-wave $D^{(*)}N$ molecular states, Int. J. Mod. Phys. Conf. Ser. **29**, 1460220 (2014).

[43] D. Zhang, D. Yang, X. F. Wang, and K. Nakayama, Possible S-wave $ND^{(*)}$ and $N\bar{B}^{(*)}$ bound states in a chiral quark model, arXiv:1903.01207.

[44] B. Wang, L. Meng, and S. L. Zhu, $D^{(*)}N$ interaction and the structure of $\Sigma_c(2800)$ and $\Lambda_c(2940)$ in chiral effective field theory, Phys. Rev. D **101**, 094035 (2020).

[45] L. Meng, B. Wang, G. J. Wang, and S. L. Zhu, Chiral perturbation theory for heavy hadrons and chiral effective field theory for heavy hadronic molecules, arXiv:2204.08716.

[46] S. Q. Luo, B. Chen, Z. W. Liu, and X. Liu, Resolving the low mass puzzle of $\Lambda_c(2940)^+$, Eur. Phys. J. C **80**, 301 (2020).

[47] K. Heikkila, S. Ono, and N. A. Tornqvist, Heavy $c\bar{c}$ and $b\bar{b}$ quarkonium states and unitarity effects, Phys. Rev. D **29**, 110 (1984).

[48] S. Ono and N. A. Tornqvist, Continuum mixing and coupled-channel effects in $c\bar{c}$ and $b\bar{b}$ quarkonium, Z. Phys. C **23**, 59 (1984).

[49] S. Ono, A. I. Sanda, N. A. Tornqvist, and J. Lee-Franzini, Where are the $B\bar{B}$ Mixing Effects Observable in the Υ Region?, Phys. Rev. Lett. **55**, 2938 (1985).

[50] S. Ono, A. I. Sanda, and N. A. Tornqvist, B meson production between the Υ (4s) and Υ (6s) and the possibility of detecting $B\bar{B}$ mixing, Phys. Rev. D **34**, 186 (1986).

[51] B. Silvestre- Brac and C. Gignoux, Unitary effects in spin orbit splitting of P wave baryons, Phys. Rev. D **43**, 3699 (1991).

[52] N. A. Tornqvist and P. Zenczykowski, Ground-state baryon mass splittings from unitarity, Phys. Rev. D **29**, 2139 (1984).

[53] M. R. Pennington and D. J. Wilson, Decay channels and charmonium mass shifts, Phys. Rev. D **76**, 077502 (2007).

[54] T. Barnes and E. S. Swanson, Hadron loops: General theorems and application to charmonium, Phys. Rev. C **77**, 055206 (2008).

[55] Z. Y. Zhou and Z. Xiao, Hadron loops effect on mass shifts of the charmed and charmed-strange spectra, Phys. Rev. D **84**, 034023 (2011).

[56] I. V. Danilkin and Y. A. Simonov, Dynamical Origin and the Pole Structure of X(3872), Phys. Rev. Lett. **105,** 102002 (2010).

[57] B. Q. Li, C. Meng, and K. T. Chao, Coupled-channel and screening effects in charmonium spectrum, Phys. Rev. D **80,** 014012 (2009).

[58] Z. W. Liu, W. Kamleh, D. B. Leinweber, F. M. Stokes, A. W. Thomas, and J. J. Wu, Hamiltonian Effective Field Theory Study of the $N^*(1535)$ Resonance in Lattice QCD, Phys. Rev. Lett. **116,** 082004 (2016).

[59] Z. W. Liu, W. Kamleh, D. B. Leinweber, F. M. Stokes, A. W. Thomas, and J. J. Wu, Hamiltonian effective field theory study of the $N^*(1440)$ resonance in lattice QCD, Phys. Rev. D **95,** 034034 (2017).

[60] Z. W. Liu, J. M. M. Hall, D. B. Leinweber, A. W. Thomas, and J. J. Wu, Structure of the $\Lambda(1405)$ from Hamiltonian effective field theory, Phys. Rev. D **95,** 014506 (2017).

[61] J. J. Wu, D. B. Leinweber, Z. W. Liu, and A. W. Thomas, Structure of the Roper resonance from lattice QCD Constraints, Phys. Rev. D **97,** 094509 (2018).

[62] O. Zhang, C. Meng, and H. Q. Zheng, Ambiversion of X (3872), Phys. Lett. B **680,** 453 (2009).

[63] P. G. Ortega, D. R. Entem, and F. Fernandez, Molecular structures in charmonium spectrum: The XYZ puzzle, J. Phys. G **40,** 065107 (2013).

[64] P. G. Ortega, J. Segovia, D. R. Entem, and F. Fernandez, Coupled channel approach to the structure of the $X(3872)$, Phys. Rev. D **81,** 054023 (2010).

[65] S. Q. Luo, B. Chen, X. Liu, and T. Matsuki, Predicting a new resonance as charmed-strange baryonic analog of $D_{s0}^*(2317)$, Phys. Rev. D **103,** 074027 (2021).

[66] D. S. Hwang and D. W. Kim, Mass of $D_{sJ}^*(2317)$ and coupled-channel effect, Phys. Lett. B **601,** 137 (2004).

[67] E. van Beveren and G. Rupp, Observed $D_s(2317)$ and Tentative $D(2100 - 2300)$ as the Charmed Cousins of the Light Scalar Nonet, Phys. Rev. Lett. **91,** 012003 (2003).

[68] Y. Tan and J. Ping, $D_{s0}^*(2317)$ and $D_{s1}(2460)$ in an unquenched quark model, arXiv:2111.04677.

[69] Z. Yang, G. J. Wang, J. J. Wu, M. Oka, and S. L. Zhu, Novel Coupled Channel Framework Connecting the Quark Model and Lattice QCD for the Near-threshold D_s States, Phys. Rev. Lett. **128,** 11 (2022).

[70] S. Weinberg, Evidence that the deuteron is not an elementary particle, Phys. Rev. **137,** B672 (1965).

[71] F. K. Guo, C. Hanhart, U. G. Meißner, Q. Wang, Q. Zhao, and B. S. Zou, Hadronic molecules, Rev. Mod. Phys. **90,** 015004 (2018).**94,** 029901(E) (2022).

[72] Y. S. Kalashnikova, Coupled-channel model for charmonium levels and an option for X(3872), Phys. Rev. D **72,** 034010 (2005).

[73] N. A. Tornqvist, Understanding the scalar meson $q\bar{q}$ nonet, Z. Phys. C **68,** 647 (1995).

[74] E. Eichten, K. Gottfried, T. Kinoshita, K. D. Lane, and T. M. Yan, Charmonium: The model, Phys. Rev. D **17,** 3090 (1978).

[75] I. V. Danilkin and Y. A. Simonov, Channel coupling in heavy quarkonia: Energy levels, mixing, widths and new states, Phys. Rev. D **81,** 074027 (2010).

[76] Y. Lu, M. N. Anwar, and B. S. Zou, How large is the contribution of excited mesons in coupled-channel effects?, Phys. Rev. D **95,** 034018 (2017).

[77] M. N. Anwar, Y. Lu, and B. S. Zou, $\chi_b(3P)$ multiplet revisited: Hyperfine mass splitting and radiative transitions, Phys. Rev. D **99,** 094005 (2019).

[78] P. G. Ortega, J. Segovia, D. R. Entem, and F. Fernandez, The $D_{s0}(2590)^+$ as the dressed $c\bar{s}(2^1S_0)$ meson in a coupled-channels calculation, Phys. Lett. B **827,** 136998 (2022).

[79] P. G. Ortega, D. R. Entem, and F. Fernández, Does the $J^{PC} = 1^{+-}$ counterpart of the $X(3872)$ exist? Phys. Lett. B **829,** 137083 (2022).

[80] P. G. Ortega, J. Segovia, D. R. Entem, and F. Fernández, Threshold effects in P-wave bottom-strange mesons, Phys. Rev. D **95,** 034010 (2017).

[81] T. Yoshida, E. Hiyama, A. Hosaka, M. Oka, and K. Sadato, Spectrum of heavy baryons in the quark model, Phys. Rev. D **92,** 114029 (2015).

[82] W. Roberts and M. Pervin, Heavy baryons in a quark model, Int. J. Mod. Phys. A **23,** 2817 (2008).

[83] N. Isgur and G. Karl, P-wave baryons in the quark model, Phys. Rev. D **18,** 4187 (1978).

[84] N. Isgur and G. Karl, Positive parity excited baryons in a quark model with hyperfine interactions, Phys. Rev. D **19,** 2653 (1979); **23,** 817(E) (1981).

[85] E. Hiyama, Y. Kino, and M. Kamimura, Gaussian expansion method for few-body systems, Prog. Part. Nucl. Phys. **51,** 223 (2003).

[86] E. Hiyama, Gaussian expansion method for few-body systems and its applications to atomic and nuclear physics, Prog. Theor. Exp. Phys. **2012,** 01A204 (2012).

[87] S. Weinberg, Phenomenological Lagrangians, Physica (Amsterdam) **96A,** 327 (1979).

[88] J. Gasser and H. Leutwyler, Chiral perturbation theory to one loop, Ann. Phys. (N.Y.) **158,** 142 (1984).

[89] S. Scherer and M. R. Schindler, *A Primer for Chiral Perturbation Theory*, Lecture Notes in Physics Vol. 830 (Springer Berlin, Heidelberg, 2012).

[90] X. W. Kang, J. Haidenbauer, and U. G. Meißner, Antinucleon-nucleon interaction in chiral effective field theory, J. High Energy Phys. 02 (2014) 113.

[91] V. Bernard, N. Kaiser, and U. G. Meissner, Chiral dynamics in nucleons and nuclei, Int. J. Mod. Phys. E **04,** 193 (1995).

[92] E. Epelbaum, H. W. Hammer, and U. G. Meissner, Modern theory of nuclear forces, Rev. Mod. Phys. **81,** 1773 (2009).

[93] U. G. Meißner, A new tool in nuclear physics: Nuclear lattice simulations, Nucl. Phys. News **24,** 11 (2014).

[94] U. G. Meißner, The long and winding road from chiral effective Lagrangians to nuclear structure, Phys. Scr. **91,** 033005 (2016).

[95] R. Machleidt and F. Sammarruca, Can chiral EFT give us satisfaction?, Eur. Phys. J. A **56,** 95 (2020).

[96] Z. W. Liu, N. Li, and S. L. Zhu, Chiral perturbation theory and the $\bar{B}\bar{B}$ strong interaction, Phys. Rev. D **89,** 074015 (2014).

[97] H. Xu, B. Wang, Z. W. Liu, and X. Liu, DD^* potentials in chiral perturbation theory and possible molecular states, Phys. Rev. D **99,** 014027 (2019).

[98] B. Wang, Z. W. Liu, and X. Liu, $\bar{B}^{(*)}\bar{B}^{(*)}$ interactions in chiral effective field theory, Phys. Rev. D **99,** 036007 (2019).

[99] H. Xu, Study of the hidden charm $D\bar{D}^*$ interactions in chiral effective field theory, Phys. Rev. D **105,** 034013 (2022).

[100] L. Meng, B. Wang, G. J. Wang, and S. L. Zhu, Hidden charm pentaquark states and $\Sigma_c^{(*)}\bar{D}^{(*)}$ interaction in chiral perturbation theory, in *Hadron Spectroscopy and Structure* (World Scientific, Singapore, 2020).

[101] L. Meng, B. Wang, and S. L. Zhu, $\Sigma_c N$ interaction in chiral effective field theory, Phys. Rev. C **101,** 064002 (2020).

[102] B. Wang, L. Meng, and S. L. Zhu, Hidden-charm and hidden-bottom molecular pentaquarks in chiral effective field theory, J. High Energy Phys. 11 (2019) 108.

[103] B. Wang, L. Meng, and S. L. Zhu, Spectrum of the strange hidden charm molecular pentaquarks in chiral effective field theory, Phys. Rev. D **101,** 034018 (2020).

[104] K. Chen, B. L. Huang, B. Wang, and S. L. Zhu, $\Sigma_c\Sigma_c$ interactions in chiral effective field theory, arXiv:2204.13316.

[105] L. Meng, B. Wang, G. J. Wang, and S. L. Zhu, The hidden charm pentaquark states and $\Sigma_c\bar{D}^{(*)}$ interaction in chiral perturbation theory, Phys. Rev. D **100,** 014031 (2019).

[106] S. Weinberg, Nuclear forces from chiral Lagrangians, Phys. Lett. B **251,** 288 (1990).

[107] S. Weinberg, Effective chiral Lagrangians for nucleon-pion interactions and nuclear forces, Nucl. Phys. **B363,** 3 (1991).

[108] V. Bernard, N. Kaiser, J. Kambor, and U. G. Meissner, Chiral structure of the nucleon, Nucl. Phys. **B388,** 315 (1992).

[109] M. B. Wise, Chiral perturbation theory for hadrons containing a heavy quark, Phys. Rev. D **45,** R2188 (1992).

[110] G. Burdman and J. F. Donoghue, Union of chiral and heavy quark symmetries, Phys. Lett. B **280,** 287 (1992).

[111] T. M. Yan, H. Y. Cheng, C. Y. Cheung, G. L. Lin, Y. C. Lin, and H. L. Yu, Heavy quark symmetry and chiral dynamics, Phys. Rev. D **46,** 1148 (1992); **55,** 5851(E) (1997).

[112] A. V. Manohar and M. B. Wise, Heavy quark physics, Cambridge Monogr. Part. Phys., Nucl. Phys., Cosmol. **10,** 1 (2000).

[113] R. Machleidt, K. Holinde, and C. Elster, The bonn meson exchange model for the nucleon nucleon interaction, Phys. Rep. **149,** 1 (1987).

[114] K. Holinde and R. Machleidt, Effect of the $\Delta(1236)$ resonance on NN scattering, nuclear matter and neutron matter, Nucl. Phys. **A280,** 429 (1977).

[115] H. Krebs, E. Epelbaum, and U. G. Meissner, Nuclear forces with Δ excitations up to next-to-next-to-leading order, part I: Peripheral nucleon-nucleon waves, Eur. Phys. J. A **32,** 127 (2007).

[116] E. Epelbaum, H. Krebs, and U. G. Meissner, Δ excitations and the three-nucleon force, Nucl. Phys. **A806,** 65 (2008).

[117] N. Kaiser, S. Gerstendorfer, and W. Weise, Peripheral NN scattering: Role of delta excitation, correlated two-pion and vector meson exchange, Nucl. Phys. **A637,** 395 (1998).

[118] T. R. Hemmert, B. R. Holstein, and J. Kambor, Chiral Lagrangians and $\Delta(1232)$ interactions: Formalism, J. Phys. G **24,** 1831 (1998).

[119] L. Micu, Decay rates of meson resonances in a quark model, Nucl. Phys. **B10,** 521 (1969).

[120] A. Le Yaouanc, L. Oliver, O. Pene, and J. C. Raynal, Naive quark pair creation model of strong interaction vertices, Phys. Rev. D **8,** 2223 (1973).